Portland State University
PDXScholar

Chemistry Faculty Publications and Presentations   Chemistry

7-1-2008

Seminaphthofluorones are a family of water-soluble, low molecular weight, NIR-emitting fluorophores

Youjun Yang

Mark Lowry

Xiangyang Xu

Jorge O. Escobedo

Martha Sibrian-Vazquez
Portland State University

See next page for additional authors

Let us know how access to this document benefits you.

Follow this and additional works at: http://pdxscholar.library.pdx.edu/chem_fac

Part of the Other Chemistry Commons

Citation Details

Authors

Youjun Yang, Mark Lowry, Xiangyang Xu, Jorge O. Escobedo, Martha Sibrian-Vazquez, Lisa Wong, Corin M. Schowalter, Timothy J. Jensen, Frank R. Fronczek, Isiah M. Warner, and Robert M. Strongin

Seminaphthofluorones are a family of water-soluble, low molecular weight, NIR-emitting fluorophores

Youjun Yang*, Mark Lowry*, Xiangyang Xu*, Jorge O. Escobedo†, Martha Sibrian-Vazquez†, Lisa Wong*, Corin M. Schowalter*, Timothy J. Jensen*, Frank R. Fronczek*, Isiah M. Warner*, and Robert M. Strongin†‡

*Department of Chemistry, Louisiana State University, Baton Rouge, LA 70803; and †Department of Chemistry, Portland State University, Portland, OR 97201

A readily accessible new class of near infrared (NIR) molecular probes has been synthesized and evaluated. Specific fluorophores in this unique xanthene based regioisomeric seminaphthofluorone dye series exhibit a combination of desirable characteristics including (*i*) low molecular weight (339 amu), (*ii*) aqueous solubility, and (*iii*) dual excitation and emission from their fluorescent neutral and anionic forms. Importantly, systematic changes in the regiochemistry of benzannulation and the ionizable moieties afford (*iv*) tunable deep-red to NIR emission from anionic species and (*v*) enhanced Stokes shifts. Anionic SNAFR-6, exhibiting an unusually large Stokes shift of ≈200 nm (5,014 cm⁻¹) in aqueous buffer, embodies an unprecedented fluorophore that emits NIR fluorescence when excited in the blue/green wavelength region. The successful use of SNAFR-6 in cellular imaging studies demonstrates proof-of-concept that this class of dyes possesses photophysical characteristics that allow their use in practical applications. Notably, each of the new fluorophores described is a minimal template structure for evaluation of their basic spectral properties, which may be further functionalized and optimized yielding concomitant improvements in their photophysical properties.

NIR dyes | xanthenes

Dyes active in the near infrared (NIR) region (>700 nm) have been under development since the first discovery of dyes with such spectral properties in the early twentieth century. NIR dyes have found wide applicability in optical recording, thermal writing displays, laser printers, laser filters, infrared photography, photodynamic therapy, and numerous other applications (1). More recently, NIR dyes have attracted considerable attention for biological and biomedical applications (2) because of inherent advantages, such as minimal interfering absorption and fluorescence from biological samples, inexpensive laser diode excitation, reduced scattering, and enhanced tissue penetration depth. Surprisingly, only a relatively few classes of NIR dyes, such as the phthalocyanines, cyanines, and squaraines, are available for use in these fields. Each of these classes of dyes has its own distinct advantages and disadvantages; moreover, common limitations include relatively small Stokes shifts and incompatibility with common fluorophores for multiplexing applications. Clearly, there is a strong need and interest in enriching the available pool of NIR fluorophores.

Annulation has proven to be quite successful for effecting bathochromic shifts through extension of the conjugated system of various dye architectures (3–4). Lee *et al.* (3) first synthesized the red-shifted type [c] naphthofluorescein framework nearly two decades ago. In addition, seminaphthofluorescein (SNAFL) and seminaphthorhodafluor (SNARF) with type [c] annulations, as developed by Haugland and coworkers (4), are in wide use today. These dyes primarily display red-shifted emissions that have maxima in the red spectral region. Importantly, although the use of type [c] annulation has proven successful at extending the emission maxima, it has not added to the pool of NIR fluorophores with emissions >700 nm.

The direction of annulation is expected to be an important variable in determining the spectral properties of xanthene based dyes. Lee *et al.* (3) suggested the possibility of two additional type [a] and [b] regioisomers. Based on semiempirical calculations, Wolfbeis and coworkers (5) predicted that the theoretical benzo [a] and benzo [b] isomers would absorb and emit at significantly longer wavelength compared with the known type [c] isomers. These studies suggest that the benzo [a, b] isomers would be interesting targets for synthesis of novel NIR fluorophores. In related work, Murata *et al.* (6) recognized that the direction of annulation plays an important role in influencing the spectral properties of a series of different benzannulated coumarins. It is notable that the linearly annulated benzo[c]coumarins displayed the shortest absorption maxima (≈335 nm) and longest emission maxima (≈540 nm), resulting in a remarkably large Stokes shift of ≈11,000 cm⁻¹ (≈200 nm).

This study addresses the relative lack of simple, readily available and practical classes of near infrared active probes, via a systematic investigation of fundamental design principles. Based on both prior theoretical (5) and experimental studies (6–8) of related molecules, we propose that a judicious variation of basic architectural features of benzannulated fluorones can reveal guiding principles for the design of next-generation NIR dyes. This hypothesis has promoted the development of a new series of seminaphthofluorones (SNAFRs), which exhibit distinct fluorescence in the deep-red to NIR spectral region. A new strategy for the synthesis of xanthene dyes (9) enables the variation of design elements, such as the direction of annulation and the regiochemistry of ionizable moieties. The resultant fluorophores display advantageous properties, such as low molecular weight, aqueous solubility, ready synthetic access, suppressed aggregation, and low cytotoxicity. Seemingly minor structural variations afford dramatic changes and unique photophysical properties. During this work, we observed appreciable NIR emissions from the SNAFR anions (emission maxima ranging from 713 to 757 nm in aqueous solution and 725–789 nm in DMSO) for three combinations of the above mentioned design variables. Most interestingly, a new compound (SNAFR-**6**) was observed to exhibit unprecedented NIR fluorescence emission when excited in the blue/green wavelength region via a Stokes shift of ≈200 nm (5,014 cm⁻¹).

Results

In an evaluation of novel NIR fluorophores and to further investigate the effect of annulation on spectral properties of
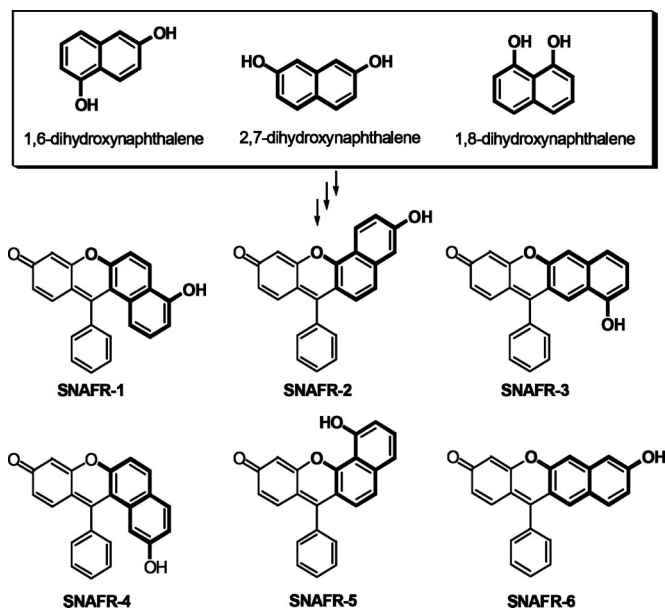
CHEMISTRY

Fig. 1. Six possible regioisomers of the SNAFR family. The detailed synthesis and characterization of the new SNAFRs and their intermediates are found in *supporting information (SI) Text*, Scheme S1, Table S1, and Figs. S1–S31. SNAFR-**1** and -**4** are classified as type [a], -**2** and -**5** are classified as type [c], and -**3** and -**6** are classified as type [b] angular and linear benzannulations based on International Union of Pure and Applied Chemistry nomenclature.

Fig. 2. Spectral properties of SNAFRs in DMSO with 1% 50 mM phosphate buffer at various pH values. Excitation emission matrices (EEMs) and absorption spectra as the pH of the added phosphate buffer was varied are provided in Figs. S32 and S34.

benzannulated xanthene dyes, we recently designed and synthesized SNAFRs **1–3**, using 1,6-dihydroxynaphthalene as the starting material (Fig. 1) (7–8). We found that type [c] angular SNAFR-**2** displayed red, green, and blue emission bands in DMSO with small amounts of added buffer, resulting in near-white light with UV excitation (8). The type [a] angular architecture SNAFR-**1** was observed to emit in the blue, orange, and near-infrared region in DMSO. In previous studies (7, 8), the direction of annulation was explored as the primary structural variable. We have recently recognized that other dihydroxynaphthalenes, such as 2,7- or 1,8-dihydroxynaphthalene may be used for the synthesis of related structural isomers. Through this approach, three new benzoxanthene architectures, SNAFRs **4–6**, are produced, thus completing a family of SNAFR isomers. Spectral properties of each of these new architectures are reported herein. These new targets possess a similar degree of conjugation between their donor and acceptor functionality and, hence, are also expected to exhibit long wavelength absorption and emission. SNAFRs **4–6** are the structural isomers of SNAFRs **1–3** with the hydroxyl donor on the naphthalene ring located at the corresponding *meta* position. These new dyes allow an investigation of a new structural variable, i.e., regiochemistry of the hydroxyl moiety.

General Spectral Properties. SNAFR-**1** has only been reported to "display blue, orange and NIR emission with UV excitation" (8). Detailed spectral properties are reported herein. The spectral properties of SNAFR-**2** are reported in refs. 7 and 8, and some spectral data are adapted from this previous publication for direct comparison with the new fluorophores. The synthesis of SNAFR-**3** is described in ref. 7. However, its spectral properties have not been reported. We note that SNAFR-**3** displays complex spectral and physical properties. For example, although its anionic form displays significant long wavelength absorption (Fig. S32C1), it does not have the expected appreciable long wavelength emission (Fig. S33). Additionally, it exhibits poor solubility in 0.1 M NaOH despite the presence of an acidic
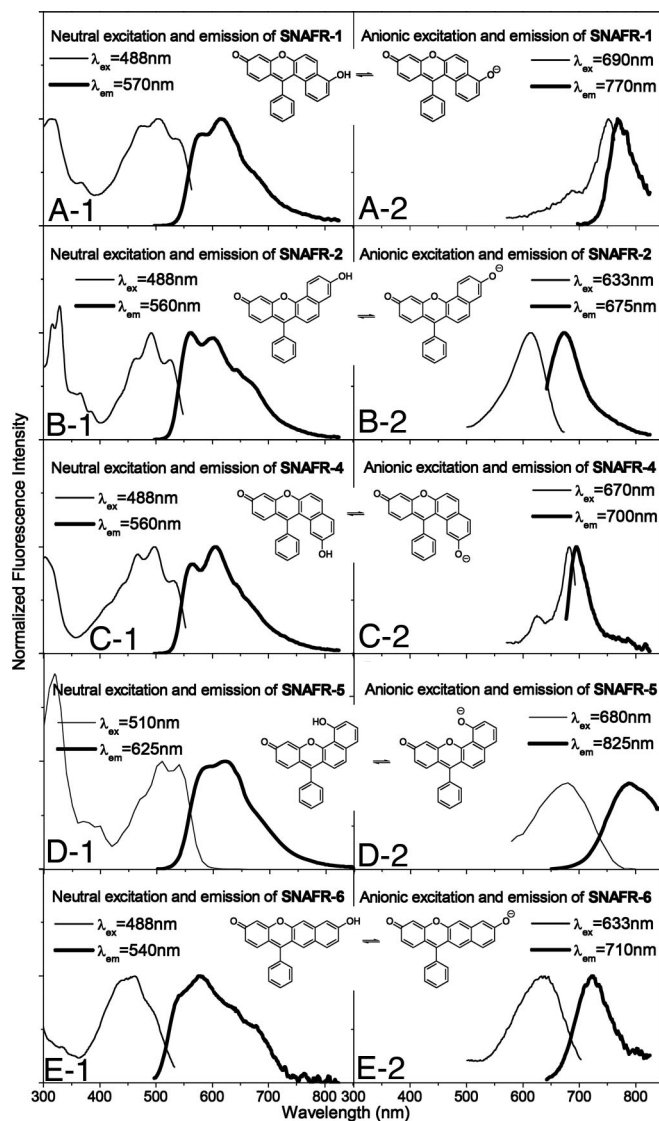
hydroxyl group. Interestingly, illumination with 365 nm light from a portable UV lamp appears to promote the solubility of SNAFR-**3** and leads to the appearance of green fluorescence. The unusual properties of SNAFR-**3** compared with the remaining five SNAFRs we have synthesized led us to exclude it from further discussion here. Thus, we will not directly compare the spectral properties of SNAFR-**3** and SNAFR-**6**, both of which have a benzo [b] framework. Further investigations is needed to better understand the complex behavior of SNAFR-**3**.

Spectral Properties of SNAFRs in DMSO with 1% Phosphate Buffer. In ref. 7, we reported the dual emission properties of the neutral and anionic forms of SNAFR-**2** in DMSO with added buffer. Such is also true for SNAFR-**1** and the newly developed SNAFRs **4–6** (Fig. 2). The neutral forms of the above five SNAFRs display strikingly similar spectral properties. Their absorption (and/or excitation) spectra display vibronic structure with their emissions generally following a mirror image relationship. Absorption maxima are located near 475 nm, with emission maxima near 600 nm. The change of either structural

Yang *et al.*

Table 1. Spectral properties of SNAFRs related to changes in structural variables

Compound		SNAFR-5		SNAFR-2		SNAFR-1		SNAFR-4		SNAFR-6 [§]
Structure										
		Same annulation: type [c] Different location of OH⁻		Same 1,6-dihydroxynaphthalene Type [c] vs. Type [a]				Same annulation: type[a] Different location of OH⁻		Same 2,7-dihydroxynaphthalene Type [a] vs. Type [b]
DMSO[†] (N)	λ_{em}	593, **621**, 641	>	**561**, 601, 646	<	583, **616**, 645	>	564, **606**, 646	>	543, **581**, 639
	λ_{abs}	464, **505**, 535	>	466, **493**, 527	<	478, **506**, 539	>	470, **498**, 532	>	440, **462**, 495
	$\Delta\lambda$	116 (3699 cm⁻¹)	>	68 (2459cm⁻¹)	<	110 (3529cm⁻¹)	~	108 (3579cm⁻¹)	<	119 (4433cm⁻¹)
DMSO[†] (A)	λ_{em}	**789**	>	**673**	<	**768**	>	**694**	<	**725**
	λ_{abs}	**676**	>	**614**	<	**747**	>	**680**	>	**637**
	$\Delta\lambda$	113 (2119 cm⁻¹)	>	59 (1428cm⁻¹)	>	21 (366 cm⁻¹)	>	14 (297cm⁻¹)	<	88 (1905cm⁻¹)
Aq.[‡] (A)	λ_{em}	**757**	>	**629**	<	**713**	>	**653**	<	**733**
	λ_{abs}	**591**	>	**542**	<	**670**	>	**630**	>	**536**
	$\Delta\lambda$	166 (3710 cm⁻¹)	>	87 (2552cm⁻¹)	>	43 (900cm⁻¹)	>	23 (559cm⁻¹)	<	197 (5014cm⁻¹)

N and A represent the *neutral* and *anionic* forms, respectively. Peak locations, including those of local maxima resulting from vibronic structure, are listed. Global maxima are shown in bold. Units are in nanometers unless otherwise noted.
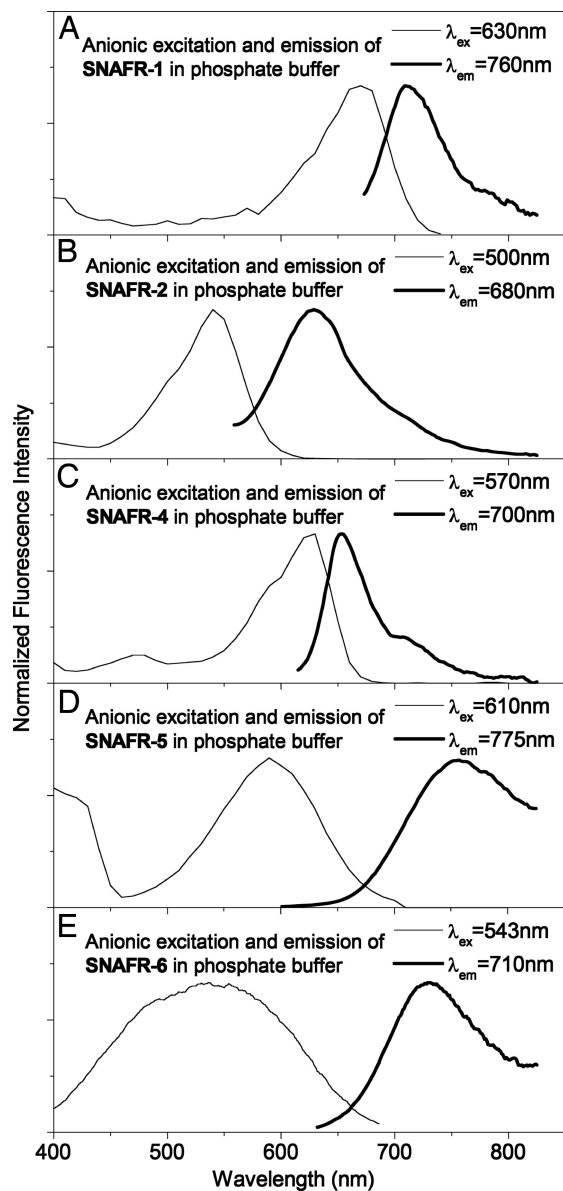[†]DMSO with 1% 50 mM phosphate buffer.
[‡]Aqueous buffer with 1% DMSO.
[§]Anionic SNAFR-6 has an estimated quantum yield of 0.09 in DMSO as referenced to rhodamine 6G in EtOH. The pK_a of SNAFR-6 in aqueous solution is calculated to be 8.18 or 8.08 based on absorption or fluorescence titrations, respectively. Isosbestic points of SNAFR-6 in aqueous solution are 380 nm and 474 nm (see Fig. S40). Exposure of anionic SNAFR-6 in aqueous solution to excitation light from a 450-W arc lamp lead to insignificant fluorescence bleaching (<2% in 1 h). A fluorescein solution under the same conditions lead to 30% bleaching (see Fig. S31 and Table S2 for details).

variable, orientation of naphthalene moiety, or the position of the hydroxyl donor does not lead to substantial spectral changes of the neutral forms (Fig. 2 and Table 1).

In contrast to the neutral forms, the spectral properties of SNAFR anions are greatly affected by both the orientation of the naphthalene moiety and location of hydroxyl group (Fig. 2 and Table 1). Anions display relatively broad and featureless peaks. SNAFR-5 displays the longest wavelength NIR emission at 789 nm, followed by SNAFR-1 at 768 nm and SNAFR-6 at 725 nm. The anionic emission of SNAFR-4 is near the interface of deep-red and NIR. The known type [c] SNAFR-2 displays the shortest wavelength emission (673 nm) of the family. The NIR emission peaks of SNAFR-1, -5 and -6 extend beyond the sensitivity of the photomultiplier tube (PMT) used for detection in this study.

The spectral properties of the N (neutral) and A (anionic) forms of SNAFR-1, -2, -4, -5, and -6 in DMSO are summarized in Table 1. In addition, a discussion of absorption acid-base titrations of SNAFRs in DMSO with 1% buffer at various pH values (Fig. S32) is provided in *SI Text*. Because of complex equilibria involving the solvolysis adduct, molar absorptivities of the SNAFRs are not reported. However, the apparent molar absorptivities of the neutral forms in DMSO (not considering the various equilibria) range from nearly 10,000 liters·mol⁻¹·cm⁻¹ to much more than 35,000 liters·mol⁻¹·cm⁻¹ with an average of ≈17,000 liters·mol⁻¹·cm⁻¹, suggesting that these compounds exhibit modest molar absorptivities. Quantum yields of the SNAFRs are modest. For example, the anion of SNAFR-6 has a quantum yield of 0.09. However, complications such as solvolysis adduct formation and modest quantum yields can be easily addressed in the next generation fluorophores by functionalization of the *ortho* position of the lower phenyl ring with groups such as carboxyl, methyl, etc. Increased steric hindrance at the central carbon will inhibit the formation of the solvent adduct. Furthermore, rotation of the phenyl ring, leading to the relaxation of excited states, will be greatly suppressed (10).

Spectral Properties of the SNAFRs in Phosphate Buffer or Aqueous Base with 1% DMSO. Stock solutions of SNAFRs in DMSO, added to phosphate buffer to obtain a dye solution in H₂O:DMSO = 99:1 (vol/vol), show good solubility, with the exception of the unusual SNAFR-3 and, to a much lesser extent, SNAFR-5. Aqueous base (0.1M NaOH) easily solubilizes SNAFR-5, which may exhibit a higher pK_a compared with the other isomers because of hydrogen bonding between the hydroxyl and the bridging xanthene oxygen. The spectral properties of the anionic forms of SNAFR-1, -2, -4, -5, and -6 in aqueous solutions with 1% DMSO are displayed in Fig. 3 and summarized in Table 1.

Anionic emission maxima of the SNAFRs in aqueous solution with 1% DMSO are observed in the red to NIR spectral regions in increasing order from SNAFR-2 (629 nm) → SNAFR-4 (653 nm) → SNAFR-1 (713 nm) → SNAFR-6 (733 nm) → SNAFR-5 (757 nm). Note that the broad SNAFR-5 and -6 emissions span beyond 850 nm (the limit of sensitivity for our PMT).

It is interesting to note that SNAFR-5 displayed the longest wavelength emission in both DMSO and aqueous solution. Although SNAFR-5 possesses many beneficial attributes, including long wavelength NIR emission and minimal if any adduct formation (data not shown), its low solubility (<0.1 mg/ml in MeOH) and difficult deprotonation in aqueous solution limit the utility of the underivatized first generation SNAFR-5 skeleton. However, SNAFR-6 displays many positive attributes, including 733 nm anionic emission in aqueous solution and minimal adduct formation (see below) without the complications that result from potential hydrogen bonding. In addition, SNAFR-6 exhibits an exceptionally large 197-nm (≈5,014 cm⁻¹) Stokes shift in phosphate buffer as a result of a large hypsochromic shift in absorption combined with a small bathochromic shift in emission. Importantly, although fluorophores with Stokes shifts >10,000 cm⁻¹ have been reported (6, 11), such an NIR-emitting fluorophore with excitation in the blue/green wavelength region is, to our knowledge, previously uncharacterized. Aggregation is ruled out as a possible explanation for this phenomenon, because the normalized absorption spectra as a function of the SNAFR-6

Fig. 3. Spectral properties of SNAFR anions studied in 50 mM phosphate buffer or aqueous base with 1% DMSO. EEMs are provided in Fig. S35.

concentration in 0.1 M NaOH are superimposable over a wide range of concentrations (Fig. S36).

Additional interest in SNAFR-**6** is derived from its comparatively small susceptibility to nucleophilic attack. We estimate that a solution of SNAFR-**6** in near neutral phosphate buffer (pH 6.92) contains ≈1% solvent adduct; i.e., nucleophilic attack at the central methine carbon by water or alcohol (8), based on the absorption spectra measured at various pH values (see Figs. S37 and S38). Although adduct formation for SNAFR-**6** is minimal at near neutral pH, it appears to be enhanced in basic buffer and in 0.1M NaOH. Apparent molar absorptivities of both majority neutral form (pH 6.92) and majority anionic (pH 9.25) SNAFR-**6** are estimated to be ≈14,000 liters·mol^{-1}·cm^{-1} without considering the various equilibria. The true molar absorptivity of the SNAFR-**6** anion is expected to be significantly greater in the absence of adduct formation. Because the NIR-emitting SNAFR-**6** scaffold (*i*) undergoes a smaller degree of solvolysis than NIR-emitting SNAFR-**1** (8) (the SNAFR-**6** chromophore is more planar compared with SNAFR-**1** and

SNAFR-**4** and therefore less reactive than these latter structures; see Fig. S31 for single crystal x-ray analysis), (*ii*) deprotonation is not diminished by potential hydrogen bonding between the hydroxyl and the bridging xanthene oxygen, and (*iii*) has other characteristics that allow it to be readily used in practical applications (see below), it is the focus of more detailed discussion in the present work. Additional spectral characterization is provided in Table S2 and Figs. S39–S41.

The SNAFR-**6** anion can be excited by using common visible laser lines and emits in the NIR region, which makes SNAFR-**6** particularly attractive for multiplexing applications. Generally, for multiplexing applications, fluorophores should possess common excitation, but distinct emission wavelengths. A current technical challenge is the lack of red or NIR emitting dyes that have large enough Stokes shifts, which allow for simultaneous excitation with common fluorophores, such as fluorescein, rhodamine, coumarin, and BODIPY dyes. SNAFR-**6** is an attractive candidate for such an application as a result of its broad anionic absorption from ≈420 nm to ≈650 nm in combination with its exceptionally large (≈200-nm) Stokes shift for a NIR emitting fluorophore. The neutral form of SNAFR-**6** is also fluorescent (emission maximum near 579 nm) in phosphate buffer with 1% DMSO. A common FITC excitation filter provides excitation near the 474-nm isosbestic point. Various filter sets (see Fig. S41), such as FITC (neutral form) or Texas red and Cy5™ (anionic form), may be used to isolate emissions from the respective forms, rendering SNAFR-**6** a promising fluorophore for ratiometric measurements.

Live Cell Imaging Using NIR Emission of SNAFR-6 Anion. As proof of concept for cell imaging, we explored live cell imaging, using the NIR emission of the SNAFR-**6** anion with a Texas red filter set. SNAFR-**6** readily enters HEp2 cells and displays adequate NIR fluorescence intensity (Fig. 4). Costaining with BODIPY ceramide, LysoSensor green, MitoTracker green, and ERTracker green shows that the majority of the dye signal emanates from the endoplasmic reticulum (ER) with some punctate signal associated with the lysosomes, suggesting possible partitioning into the membranes. Low cytotoxicity is also observed (see Fig. S43).

Discussion

Trends in Structure and Fluorescence Properties. We examine here the spectral properties of five members of the regioisomeric seminaphthofluorone family in two different solvent systems (DMSO with 1% aqueous base and aqueous base with 1% DMSO), thus allowing several comparisons (e.g., SNAFR -**5** and -**2**, SNAFR -**2** and -**1**, SNAFR -**1** and -**4**, and SNAFR -**4** and -**6**) of the effect of structural variables such as annulation and regiochemistry of hydroxyl donor based on different dihydroxynaphthalene starting materials. The correlation of structure and fluorescence properties of the SNAFRs is summarized in Table 1. The effect of structural variables on the spectral properties of the neutral form of SNAFRs in DMSO with 1% aqueous base is relatively modest. However, in agreement with predictions by Wolfbeis and coworkers (5), the SNAFR anions are greatly affected by orientation of the naphthyl moiety. We also find that the location of the ionizable hydroxyl group has a significant effect on spectral properties of SNAFR anions in both the relatively less (DMSO with 1% aqueous base) and more polar (aqueous base with 1% DMSO) solvent systems studied to date.

It is apparent that SNAFR-**2** exhibits notable similarities to SNAFR-**5**. These analogs possess the same type [c] annulation and differ in hydroxyl regiochemistry but have similar spectral shapes. In addition, the violet-blue fluorescence due to solvolysis adduct formation is not prominently observed in either case. Interestingly, the regiochemistry of the hydroxyl group apparently has a dramatic effect on the absorption and emission
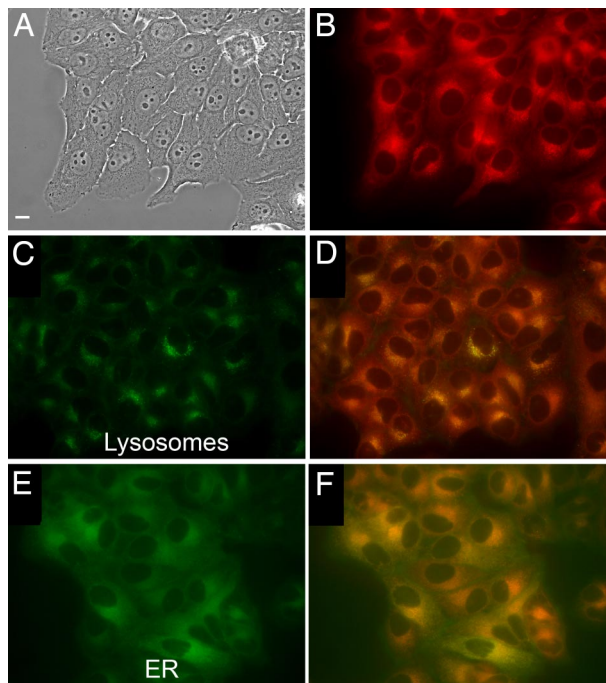
Fig. 4. HEp2 cell staining studies using SNAFR-**6**. (*A*) Phase contrast of cells stained with 10 μM SNAFR-**6**. (*B*) SNAFR-**6** Fluorescence collected with the following Texas red filter set: excitation, 540–580 nm; emission, 610 nm long pass. (*C*) Lysosomes staining with LysoSensor green. (*D*) Costaining with Lyso-Sensor green and SNAFR-**6**. (*E*) ER staining with ERTracker green. (*F*) Costaining with ERTracker Green and SNAFR-**6**. Costaining with additional probes can be found in Fig. S42. (Scale bar, 10 μm.)

maxima with SNAFR-**5** absorbing and emitting at substantially longer wavelengths compared with SNAFR-**2**. We also note that the SNAFR-**5** anion displays a much larger Stokes shift compared with the SNAFR-**2** anion.

A specific comparison of the SNAFR-**1** and -**2** anions reveals that the direction of annulation also has a dramatic effect on peak locations, with the type [a] compound absorbing and emitting at substantially longer wavelengths as predicted in ref. 5 and observed in ref. 6 for other dye structures with analogous angular annulations. It is interesting to note that the spectral features of anionic SNAFR-**2** are much broader than those of the SNAFR-**1** anion. In addition, SNAFR-**2** anion displays a larger Stokes shift than the SNAFR-**1** anion.

A comparison of SNAFR-**1** and -**4** anions, compounds with the same type [a] annulation but with varying locations of their hydroxyl moieties, shows that this second structural variable also has a large impact on properties. The absorption and emission maxima and Stokes shift of SNAFR-**1** are greater than SNAFR-**4** in both solvents. Qualitatively, their spectra appear similar (narrow peak shapes and comparatively modest Stokes shifts) with the exception of the shift to longer wavelengths observed for SNAFR-**1**.

Trends in absorption and fluorescence maxima mirror one another in the comparisons discussed above (e.g., different location of the hydroxyl for type SNAFR-**1** vs. type [a] SNAFR-**4** and type [a] vs. type [c] annulation for SNAFR-**1** vs. SNAFR-**2**; and different location of the hydroxyl for type [c] SNAFR-**2** vs. type [c] SNAFR-**5**). However, when comparing the type [a] SNAFR-**4** anion with the type [b] SNAFR-**6** anion, a change from the angularly annulated SNAFR-**4** to the linear SNAFR-**6** increases the wavelength of emission maximum while decreasing the wavelength of absorption maximum. An unusually large Stokes shift, especially in buffer (197 nm in buffer vs. 88 nm in DMSO), is the consequence. It is interesting to note that the same trends in either absorption or emission are observed for both solvents for all four SNAFR anion comparisons.

Similarly, Stokes shifts of all five SNAFR anions are greater in aqueous solution with 1% DMSO compared with what is observed in DMSO with 1% aqueous base. In addition, the anionic absorption and/or excitation maxima in buffer with 1% DMSO all display hypsochromic shifts compared with the corresponding DMSO solution with 1% aqueous base, increasing in order from SNAFR-**4** (50 nm) → SNAFR-**2** (72 nm) → SNAFR-**1** (77 nm) → SNAFR-**5** (85 nm) → SNAFR-**6** (101 nm). Hypsochromic shifts in both the absorption and emission maxima of xanthene dyes are common when changing from DMSO to aqueous solutions and are attributed to hydrogen bonding stabilization effects (12–13).

Interestingly, hypsochromic shifts are observed in the emissions of four of five SNAFRs investigated increasing in order from SNAFR-**5** (32 nm) → SNAFR-**4** (41 nm) → SNAFR-**2** (44 nm) → SNAFR-**1** (55 nm). The exception, anionic SNAFR-**6,** displays an 8-nm bathochromic shift (from 725 nm to 733 nm) in aqueous compared with DMSO solution. The large hypsochromic shift in absorption, combined with the unusual bathochromic shift in emission, produce an unusually large Stokes shift in buffer. The reason for the unusual bathochromic shift of the SNAFR-**6** emission is not clear. However, an unusually large Stokes shift was observed for a similar linearly annulated benzocoumarin in ref. 6. In that study, it was hypothesized that the emissive intramolecular charge transfer character in the excited state may have been stabilized by the solvation of polar solvents resulting in red shifted emission (6, 14). We note that solvatochromic properties of polarity sensitive dyes is a complex topic, involving many factors including the dipole moment of the ground and excited states of the solute and the dielectric constant, refractive index, and hydrogen bonding ability of the solvent (15).

It is apparent that both structural variables play a major role in determining the spectral properties of the dyes reported here. For example, the largest change in the emission of the SNAFR anions in aqueous solution was between SNAFR-**5** and -**2** (type [c] architectures with different locations of the hydroxyl), whereas the largest change in the absorption was between SNAFR-**2** and -**1** (same regiochemistry of the hydroxyl provided by 1,6-dihydroxynaphthalene with different type [c] vs. type [a] annulation). The smallest change in both the emission and absorption of the SNAFR anions in aqueous solution was between SNAFR-**1** and -**4** (type architectures with different locations of the hydroxyl). Although there is precedent in the literature for investigating the effect of annulation on spectral properties, this work adds the regiochemistry of the ionizable hydroxyl moiety, thus providing access to additional compounds with unique structural and spectral properties. Further investigations into how photophysical properties are correlated to the electronic states of the new architectural motifs should afford insights into the design of fluorophores with tunable properties, such as large Stokes shifts and red-shifted emission.

Conclusion

Extension of the initial investigations of the first generation dye prototypes reported here would afford ready access to more fluorophores with unprecedented properties. For example, introducing substituents at the *ortho* position of the lower aryl ring (see above) of the SNAFRs should effectively increase quantum yields by increasing structural rigidity and decreasing the formation of solvent adducts (10). It is also of interest to synthesize the semi-naphthorhodafluor analogs of the SNAFRs. Pioneering work in this latter area has been reported by Haugland and coworkers (4). The benefits include further red shifted absorption and emission maxima as determined by the structure of dialkylamine used, and higher quantum yields, improved photostability, reduced acid/base sensitivity and longer wavelength emission.

CHEMISTRY

In summary, the regioisomeric seminaphthofluorone (SNAFR) series displays unique spectral properties, including tunable deep-red to NIR emission for anionic species with moderate to large Stokes shifts. Synthetic methods featuring variations in both the orientation of annulation and the regiochemistry of the ionizable hydroxyl moieties have allowed for structure-function investigations, providing information that can be used for future rational design of second generation dye systems. Both of these structural variables have comparatively small effects on the spectral properties of the neutral form of SNAFRs in DMSO. In contrast, both variables produce dramatic effects on the spectral properties of SNAFR anions in both DMSO and aqueous buffer. Large differences in the properties of the specific dyes of this class result from seemingly small structural changes. The most notable example, SNAFR-**6**, combines type linear annulation with hydroxyl regiochemistry, which results in a previously uncharacterized combination of NIR emission upon excitation at its absorption maxima in the blue/green spectral region (an ≈200-nm Stokes shift). A correlation of photophysical properties to the electronic states of the new architectural motifs reported here should afford ample opportunity for further experimental and theoretical insights. These first generation prototypes are readily functionalizable generic templates embodying an alternative class of NIR-active probes that exhibit many advantageous properties including low molecular weight, aqueous solubility, simple synthetic access, suppressed aggregation, and low cytotoxicity. The combination of deep-red to NIR emission with moderate to large Stokes shifts allows for potential multiplexing with a great number of commercially available fluorophores.

Materials and Methods

General Methods. All reagents were purchased from Sigma–Aldrich and used without further purification, except for THF and CH_2Cl_2, which were dried by using the Innovative Technologies solvent purification system. EtOAc, hexane, $CHCl_3$, acetone, and MeOH were purchased from EMD Biosciences and were used as received. All reactions were performed under Ar atmosphere unless otherwise indicated. TLC was performed by using silica XHL TLC plates, (glass backed, 250 μm) (Sorbent Technologies). Column chromatography separations were done by using 60 Å silica gel with a distribution of 40–63 μm (Sorbent Technologies). Maldi-MS spectra were obtained on an Applied Biosystems QSTAR XL spectrometer. NMR spectra were acquired in DMSO-d_6 or $CDCl_3$ on Bruker DPX-250, DPX-300, or Avance-400 spectrometers. All chemical shifts are reported with DMSO referenced at 2.49 ppm for ^{1}H NMR and at 39.5 ppm for ^{13}C NMR, or with $CDCl_3$ referenced at 7.26 ppm for ^{1}H NMR and at 77.0 ppm for ^{13}C NMR.

X-Ray Crystallography. Intensity data for x-ray crystallography was collected at T = 90 K, using graphite monochromated MoKα radiation (λ = 0.71073 Å) on a Nonius KappaCCD diffractometer fitted with an Oxford Cryostream cooler. Structures were solved by direct methods and refined by full-matrix least squares, using SHELXL97 (16).

For all compounds, H atoms were visible in difference maps but were placed in idealized positions. Torsional parameters were refined for methyl groups and OH hydrogen positions were refined individually.

UV-Vis Absorption and Fluorescence Spectroscopy. UV-Vis spectra were collected with a Cary 50 Bio UV-Vis spectrophotometer at room temperature, using 1-cm quartz cuvette. Fluorescence spectra were obtained by using a Fluorolog -22Tau3 (Horiba Jobin Yvon) with a 1-cm pathlength quartz cell (Starna Cells). Emission spectra were collected after excitation with a 450 W xenon arc lamp. A dual monochromator was used to select light of 325, 488, 514, 543, and 633 nm (band pass = 1 nm). Emission wavelengths were scanned with 1-nm step sizes, using a dual monochromator (band pass = 4 nm). Integration time was set to 0.1 sec per point and 950 V was applied to a Hamamatsu R928 PMT. Excitation spectra were monitored with an emission and excitation band pass of 4 and 1 nm, respectively. All spectra were fully corrected. Excitation emission matrices (EEMs) were collected over various spectral regions, using 2-nm step sizes for emission and 10-nm step sizes for excitation. The bandpass for excitation and emission was typically 1 and 4 nm, respectively, with the excitation bandpass occasionally increased to 4 nm. An estimate of the fluorescence quantum yield was obtained as reported.

Live-Cell Measurements. HEp2 cells were obtained from ATCC and maintained in a 50:50 mixture of DMEM:Advanced MEM (Invitrogen) supplemented with 5% FBS (Invitrogen) and Primocin as antibiotic (Invivogen). Cells were subcultured twice weekly to maintain working stocks. HEp2 cells were seeded onto LabTek II chamber coverslips and allowed to grow for 48 h. SNAFR-**6** was first prepared as a 10 mM stock in DMSO and then diluted directly into medium to 10 μM. HEp2 cells were loaded overnight in medium containing 10 μM SNAFR-**6**. The next morning, the following organelle tracers (Invitrogen) were added and incubated: ERTracker green, 100 nM for 1 h for ER; MitoTracker green, 250 nM for 30 min for mitochondria; LysoSensor green, 50 nM for 30 min for lysosomes; and BODIPY ceramide 50 nM for 30 min for Golgi complex. After organelle staining, cells were washed three times and fed medium containing 50 mM Hepes (pH 7.2) and examined by using a Zeiss Axiovert 200 fluorescent microscope fitted with standard FITC and Texas red filters (Chroma Technology). Images were acquired by using a Zeiss AxioCam MRm digital camera.

Cytotoxicity Study. HEp2 cells were plated on a 96-well plate (Costar) at 7,500 cells per well and allowed to grow for 48 h. A 10 mM compound stock was diluted 100× to give a 100 μM concentration in medium that was sonicated for 30 min in a water bath sonicator. Serial twofold dilutions were then made down to 3.125 μM, and cells were loaded overnight with compound. Loading medium was then removed and replaced with medium containing Celltiter blue reagent (Promega) and incubated for 4 h. Conversion of the substrate to product was assayed by measuring the fluorescence, using a BMG FLUOstar plate reader at 570/615 nm (excitation/emission). Readings were normalized by setting 0% survival to a baseline acquired by averaging six wells treated with 0.2% saponin during the loading interval. Untreated cells were considered to be 100% viable, and the average of six wells was used to set this parameter.

Supporting Information Available. Detailed syntheses of SNAFRs **4**, -**5**, and -**6** may be found in Scheme S1 (reaction) and Scheme S2 (carbon numbering). Analysis and NMR and mass spectra of compounds **3**–**5** and **7**–**9** and SNAFRs **1**–**6** and additional costaining experiments involving SNAFR-**6**; SNAFR-**6** toxicity data may be found in SI Text. Crystallographic information for SNAFR-**4** (Cambridge Crystallographic Data Centre entry 682696) is provided in SI Text.

1. Fabian J, Nakazumi H, Matsuoka M (1992) Near-infrared absorbing dyes. *Chem Rev* 92:1197–1226.
2. Rao J, Dragulescu-Andrasi A, Yao H (2007) Fluorescence imaging *in vivo*: Recent advances. *Curr Opin Biotech* 18:17–25.
3. Lee LG, Berry GM, Chen, C-H (1989) Vita blue: A new 633-nm excitable fluorescent dye for cell analysis. *Cytometry* 10:151–164.
4. Whitaker JE, Haugland RP, Prendergast FG (1991) Spectral and photophysical studies of benzo[c]xanthene dyes: Dual emission pH sensors. *Anal Biochem* 194:330–344.
5. Fabian WMF, Schuppler S, Wolfbeis OS (1996) Effects of annulation on absorption and fluorescence characteristics of fluorescein derivatives: A computational study. *J Chem Soc Perkin Trans 2* 5:853–856.
6. Murata C, *et al.* (2005) Improvement of fluorescence characteristics of coumarins: Syntheses and fluorescence properties of 6-methoxycoumarin and benzocoumarin derivatives as novel fluorophores emitting in the longer wavelength region and their application to analytical reagents. *Chem Pharm Bull* 53:750–758.
7. Yang Y, *et al.* (2006) An organic white light-emitting fluorophore. *J Am Chem Soc* 128:14081–14092.
8. Yang Y, *et al.* (2007) An organic white light-emitting fluorophore. *J Am Chem Soc* 129:1008–1008.
9. Yang Y, *et al.* (2005) A convenient preparation of xanthene dyes. *J Org Chem* 70:6907–6912.
10. Urano Y, *et al.* (2005) Evolution of fluorescein as a platform for finely tunable fluorescence probes. *J Am Chem Soc* 127:4888–4894.
11. Yang J, *et al.* (2004) Arylethynyl substituted 9,10-anthraquinones: Tunable stokes shifts by substitution and solvent polarity. *Chem Mater* 16:3457–3468.
12. Martin MM (1975) Hydrogen bond effects on radiationless electronic transitions in xanthene dyes. *Chem Phys Lett* 35:105–111.
13. Choi MF, Hawkins P (1994) Solvatochromic studies of fluorescein dianion in *N,N*-dimethylformamide/water and dimethylsulphoxide/water mixtures. *Spectrosc Lett* 27:1049–1063.
14. Langmuir ME, Yang J-R, Moussa AM, Laura R, LeCompte KA (1995) New naphthopyranone based fluorescent thiol probes. *Tetrahedron Lett* 36:3989–3992.
15. Reichardt C (1994) Solvatochromic dyes as solvent polarity indicators. *Chem Rev* 94:2319–2358.
16. Sheldrick GM (1997) SHELXL97 (University of Göttingen, Germany).